Eur. Phys. J. Appl. Phys. **93**, 30301 (2021)

https://doi.org/10.1051/epjap/2021200366

THE EUROPEAN PHYSICAL JOURNAL APPLIED PHYSICS

Regular Article

Structural and optical properties of molybdenum oxide thin films prepared by the dip coating technique

Danial Ahmad[1,*], M. Amer Khan[2], Arslan Mahmood[3], Amjad Sohail[3], and S.S. Ali Gillani[1]

[1] Government College University, Lahore, Punjab 54000, Pakistan
[2] Comsats University Islamabad, Lahore, Punjab 54000, Pakistan
[3] Department of Physics, Government College University Faisalabad (GCUF), Allama Iqbal Road, Faisalabad 38000, Pakistan

Received: 30 November 2020 / Received in final form: 10 February 2021 / Accepted: 12 February 2021

Abstract. Due to their excellent structural and optical properties of molybdenum oxide thin films are used in various applications such as gas-sensing, solar cells, optoelectronic and medical physics. The present study is related to the synthesis of molybdenum oxide thin films prepared by dip coating technique and the films were characterized by using various techniques such as XRD, SEM and UV-visible spectroscopy. The monoclinic crystal structure and the crystallite size (29.16–52.77 nm) was investigated by X rays diffraction (XRD) analysis. SEM micrograph was used to identify the nano tubes in MoO_3 thin film and UV-visible spectroscopy exhibits the maximum absorption in ultra-violet region and band gap decrease (3.17–2.71 eV) with increased the inner transition states in molybdenum thin film. Finally, the results show that the series of molybdenum oxides MoO1 (Sample 1), MoO2 (Sample 2) and MoO3 (sample 3) exhibited interesting structural and optical properties which make them good candidates for photo catalytic activity.

1 Introduction

Air pollution is due to the various gases such as NO, NO_2 and CO_2 released from combustion processes and automobiles. These gases are extremely harmful to the human body and also the main cause of diseases. Therefore, in order to overcome and control this problem, there has been a strong demand to effective methods. Molybdenum oxide plays very important role for detecting gases such as NO [1], NO_2 [2], NH_3 [3–5], H_2 [3,6], CO [6,7] and LPG [3]. Molybdenum oxide may be the most considerable material in multiple fields due to its interesting physical and chemical properties [8] and the MoO has vast scope in different technological applications such as electro chromic [9], thermo chromic and photo chromic lens [9,10] smart window, self-developing photography, conductive gas sensors [11], photovoltaic [12], lubricant, Li-ion batteries capacitors and field effect transistors (FET) [13–15].

Molybdenum oxide can exists in three basic crystalline phase such as orthorhombic (α-MoO_3), meta stable monoclinic (β-MoO_3) and hexagonal [16,17]. In α-MoO_3 phase, bilayer structure is formed due to distortion which makes it a stratified structure. These bilayers contain a chain of MoO_6 octahedral by sharing corners and edges in particular direction and bonded with Van der Waals forces while the structure of β-MoO_3 is not layered because of corner sharing of distorted octahedral in three dimensions. The hexagonal structure of MoO_3 contain the chain of octahedral connect with corners and they make hexagonal structure in typically 1D and trigonal channels and these channels may composed of tiny ions [18–21]. Different researchers have reported that molybdenum oxides have various potential applications like, Buono-Core et al. [22] prepared the molybdenum oxide thin films by using a photochemical deposition method for gas sensing application. The prepared samples are amorphous in nature and exhibited good optical properties. Oxidation states of Mo^{+5} and Mo^{+6} were revealed by XPS study. Samples show good sensitivity toward 50 ppm NH_3 at an operating temperature of 350 °C. Uthanna et al. [23] reported that MoO_3 has excellent optical properties compared to other inorganic materials such as TiO_2 and IrO_2 due to their stronger and uniform absorption of light in the coloured state. Adhikari et al. reported that the semiconductor material shows distinctive structural and optical properties due to its smaller size [24]. Various deposition techniques have been used to prepare molybdenum oxide thin film either in amorphous or crystalline depends upon synthesis technique like sol–gel technique [25,26], electron beam evaporation [27], spray pyrolysis [9,28], radio frequency magnetron sputtering [4,29,30], pulsed laser deposition (PLD) [5,31], chemical vapour deposition (CVD) [32,33], magnetron sputter deposition (MSD) [34], spin coating [35], electrochemical deposition [36], flash and thermal evaporation [37,38], physical vapour deposition (PVD) [39], combustion chemical vapour deposition (CCVD) [40], hot filament metal oxide deposition (HFMOD) [41], metal oxide chemical vapour deposition MOCVD [42], dip coating [43].

* e-mail: danishah899@gmail.com

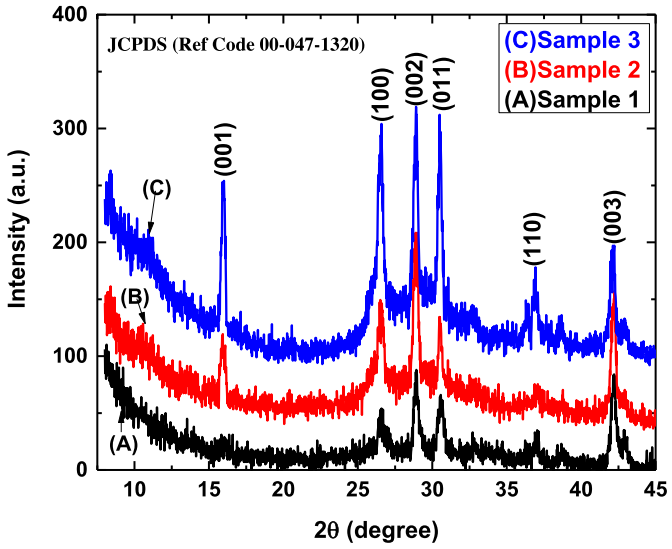

Fig. 1. XRD patterns of molybdenum oxide thin films.

In this study, molybdenum oxide thin films were synthesized by dip coating method. This technique is chosen for its low cost and because it makes it possible to deposit layers with adjustable thickness. Structural and optical properties of molybdenum oxide MoO-1 (sample 1), MoO-2 (sample 2) and MoO-3 (Sample 3) were characterized by using XRD, Scanning electron micrographs SEM and UV-visible spectroscopy.

2 Experimental procedure

2.1 Synthesis of molybdenum oxide thin films

Molybdenum oxide thin films were deposited on glass substrate by using dip coating method. Initially, 3 g of MoO_3 powder (99%, Panreac) were mixed with 20 ml of hydrogen peroxide (H_2O_2, 31%, Merck) in glass beaker. Then the solution was heated at 80 °C for 2 h and cooled at room temperature (RT) for 24 h. After that the solution was completely dissolved and yellow color obtained. Polyethylene Glycol (PEG $C_2H_4O_2$, Mn 400, and Merck) was added to solution with different ratios and heated at 70 °C for 30 min. The glass substrates were cut to an appropriate size and washed with ethanol and deionized water then dried in suitable manner to remove contamination. The samples are labeled MoO-1 (sample 1), MoO-2 (sample 2) and MoO-3 (sample 3) according to the volume ratio (MoO: PEG = 4: 1, 5: 1.25 and 7: 1.75).

2.2 Characterisation

The structure and phase confirmation of prepared samples were performed by PAN anlytical-Xpert PRO XRD, operated at: 40 kV and 40 mA using Cu Kα radiation ($\lambda \sim 0.154$ nm) with 2θ from 0° to 45°. The surface morphology was analysed by using jeol JSM-6480LV with the accelerating voltage of 20 kV. The UV visible spectroscopy was carried out on Genesys 10S UV-Vis spectrophotometer for optical analysis.

Table 1. Deposition and structural parameters of molybdenum oxide films.

Molybdenum oxide	Volume ratio (gm)	Avg. Crystallite size (nm)
Sample 1	4:1	29.16
Sample 2	5:1.25	31.02
Sample 3	7:1.75	52.77

3 Result and discussion

3.1 Structural analysis

The XRD was used to study the crystal structure and crystallite size of molybdenum oxide thin films. Figure 1 shows the monoclinic crystal structure of molybdenum oxide films series (Sample 1, Sample 2 & Sample 3), the lattice parameters as (a = 3.954 Å, b = 3.687 Å and c = 7.095 Å) and the miller indices of these diffracted peaks were expressed as (100), (002), (011) and (003) compared with standard card JCPDS (Ref Code 00-047-1320). The thickness was found about 142–216 nm. Furthermore, the average crystallite size T of the molybdenum oxide thin film were calculated by using Scherer equation (1) [44].

$$T = K\lambda/\beta\cos\theta. \quad (1)$$

Experimental and structural parameters are summarized in Table 1.

3.2 Surface morphology

The scanning electron microscopy was used to study the surface morphology of MoO thin films (Sample 1, Sample 2 & Sample 3). Figure 2 shows that SEM micrograph and the shape of the grains was needle like structured and the substrate is partially covered with grains due to low volume ratio of sample. The grains size was found about 130–180 nm. According to literature, the grains shape like oval, plates, needle, and elongated depends on the deposition techniques such as growing conditions and deposition steps of the thin films. Pachlhofer et al. [45] reported that the same results by using dc magnetron sputtering technique. As the volume ratio of molybdenum oxide constituents increases, the grains mix and cover the whole surface of the substrate (as shown in Fig. 2B). The grains are converted into nanotubes as shown in Figure 2C due to further increase in volume ratio of constituents [8].

3.3 UV-visible spectroscopy analysis

The UV-visible spectroscopy was carried out to study the optical absorbance and to determine the band gap (Eg) of molybdenum oxides films. Figure 3 shows that absorbance spectra of (A) sample 1, (B) sample 2 and (C) sample 3. The maximum absorption rates were recorded near UV region from 220 to 315 nm. The obtained results show that the peaks of absorbance spectra broaden with increasing the

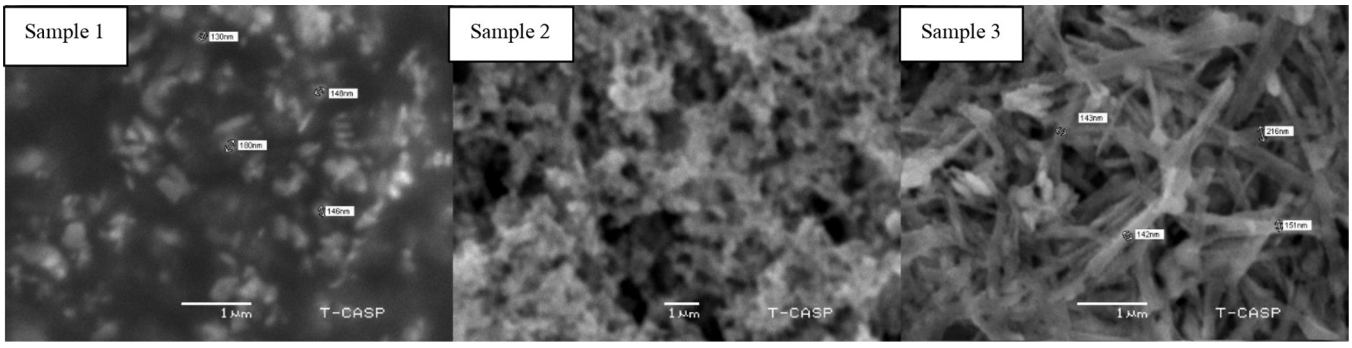

Fig. 2. SEM micrographs of (A) MoO_1 (B) MoO_2 and (C) MoO_3 thin films.

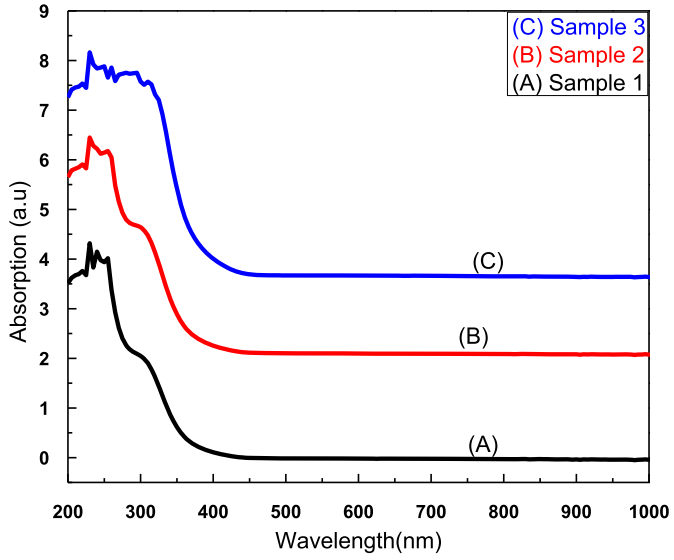

Fig. 3. Absorption spectra of molybdenum oxide thin films.

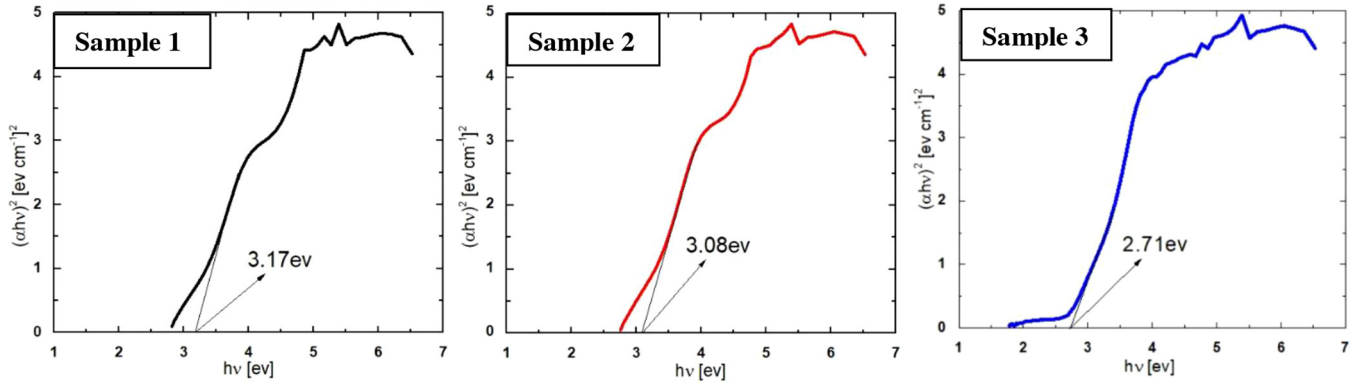

Fig. 4. Plot of $(\alpha h\nu)^2$ vs $h\nu$ of molybdenum oxide films.

volume ratios in the samples. To find the band gap of molybdenum oxide thin film "Tauc equation" [46] was used.

$$(ahv)^{1/n} = A(hv - E_g) \tag{2}$$

where, $n = 2$ for indirect band gap and $n = \frac{1}{2}$ for direct band gap. In present case the band gap is direct [15]. The energy band gap is obtained from extrapolation of straight line to the zero absorption as shown in Figure 4. Result shows that the value of energy band gap decreases from 3.17 to 2.71 eV with increase in volume ratio. The values of band gap in literature are 2.96 [47] and 3.2 eV [48] As band gap is decreasing, one may assume that by deficiency of oxygen there are some new electrons states are introduced between conduction and valence band in the structure of sample 3 [14].

4 Conclusion

The dip coating technique was used to synthesis of molybdenum oxide thin films with different volume ratio (MoO: PEG = 4:1, 5:1.25 and 7:1.75). The films were characterized by using various techniques such as XRD, SEM and UV-Visible Spectroscopy. XRD pattern confirms the monoclinic structure with β-MoO_3 phase and the crystallite size was increased from 29.16 to 52.77 nm by increasing volume ratio. Furthermore, SEM micrographs showed the growth of nano tubes and UV-VIS results indicated that the maximum absorption in ultra violet region with decreasing trend in band gap from 3.27 to 2.71 eV. It is presumed that, the decrease in the band gap is due to the formation of new energy states between the conduction and valence bands.

Author contribution statement

D. A. and S. S. A. G. conceived and designed research. D. A. synthesized and characterized the MoO thin films. D. A. and A. M. contributed to the structuring of the manuscript. M. A. K. participated in the discussion. A. S. critically revised and updated the manuscript. All the authors read the manuscript and approved its final submission.

References

1. M. Di Giulio, D. Manno, G. Micocci, A. Serra, A. Tepore, Phys. Status Solidi A **168**, 249 (1998)
2. V. Guidi, G.C. Cardinali, L. Dori, G. Faglia, M. Ferroni, G. Martinelli, P. Nelli, G. Sberveglieri, Sens. Actuators, B **49**, 88 (1998)
3. S. Sunu, E. Prabhu, V. Jayaraman, K. Gnanasekar, T. Seshagiri, T. Gnanasekaran, Sens. Actuators, B **101**, 161 (2004)
4. C. Imawan, F. Solzbacher, H. Steffes, E. Obermeier, Sens. Actuators, B **64**, 193 (2000)
5. S. Sunu, E. Prabhu, V. Jayaraman, K. Gnanasekar, T. Gnanasekaran, Sens. Actuators, B **94**, 189 (2003)
6. C. Imawan, H. Steffes, F. Solzbacher, E. Obermeier, Sens. Actuators, B **78**, 119 (2001)
7. M. Ferroni, V. Guidi, G. Martinelli, P. Nelli, M. Sacerdoti, G. Sberveglieri, Thin Solid Films **307**, 148 (1997)
8. T. Nagyné-Kovács, L. Studnicka, I.E. Lukács, K. László, P. Pasierb, I.M. Szilágyi, G. Pokol, Nanomaterials **10**, 891 (2020)
9. J. Scarminio, A. Lourenco, A. Gorenstein, Thin Solid Films **302**, 66 (1997)
10. T. He, J. Yao, J. Photochem. Photobiol., C **4**, 125 (2003)
11. D. Mutschall, K. Holzner, E. Obermeier, Sens. Actuators, B **36**, 320 (1996)
12. Y.-C. Tseng, A.U. Mane, J.W. Elam, S.B. Darling, Sol. Energy Mater. Sol. Cells **99**, 235 (2012)
13. S. Bhatia, A. Khanna, presented at the AIP Conference Proceedings, 2015 (unpublished)
14. M. Rao, K. Ravindranadh, A. Kasturi, M. Shekhawat, Res. J. Recent Sci. ISSN **2277**, 2502 (2013)
15. R. Patil, M. Uplane, P. Patil, Int. J. Electrochem. Sci. **3**, 259 (2008)
16. E.I. Altman, T. Droubay, S.A. Chambers, Thin Solid Films **414**, 205 (2002)
17. T. Ivanova, K. Gesheva, A. Szekeres, J. Solid State Electrochem. **7**, 21 (2002)
18. A. Chithambararaj, N. Rajeswari Yogamalar, A.C. Bose, Cryst. Growth Des. **16**, 1984 (2016)
19. V.V. Kumar, K. Gayathri, S.P. Anthony, Mater. Res. Bull. **76**, 147 (2016)
20. I.A. de Castro, R.S. Datta, J.Z. Ou, A. Castellanos-Gomez, S. Sriram, T. Daeneke, K. Kalantar-zadeh, Adv. Mater. **29**, 1701619 (2017)
21. I.M. Szilágyi, J. Madarász, G.r. Pokol, P. Király, G. Tárkányi, S. Saukko, J. Mizsei, A.L. Tóth, A. Szabó, K. Varga-Josepovits, Chem. Mater. **20**, 4116 (2008)
22. G. Buono-Core, A. Klahn, C. Castillo, E. Muñoz, C. Manzur, G. Cabello, B. Chornik, J. Non-Cryst. Solids **387**, 21 (2014)
23. S. Uthanna, V. Nirupama, J. Pierson, Appl. Surf. Sci. **256**, 3133 (2010)
24. T. Adhikari, D. Pathak, T. Wagner, R. Jambor, U. Jabeen, M. Aamir, J.-M. Nunzi, Opt. Mater. **73**, 70 (2017)
25. A.K. Prasad, D.J. Kubinski, P.-I. Gouma, Sens. Actuators, B **93**, 25 (2003)
26. W. Dong, B. Dunn, J. Mater. Chem. **8**, 665 (1998)
27. K. Madhuri, B. Naidu, O. Hussain, Mater. Chem. Phys. **77**, 22 (2003)
28. A. Bouzidi, N. Benramdane, A. Nakrela, C. Mathieu, B. Khelifa, R. Desfeux, A. Da Costa, Mater. Sci. Eng., B **95**, 141 (2002)
29. C. Imawan, H. Steffes, F. Solzbacher, E. Obermeier, Sens. Actuators, B **77**, 346 (2001)
30. D. Pathak, R. Bedi, D. Kaur, Surf. Rev. Lett. **16**, 917 (2009)
31. I.C. Lekshmi, A. Gayen, M. Hegde, Mater. Res. Bull. **40**, 93 (2005)
32. T. Ivanova, M. Surtchev, K. Gesheva, Mater. Lett. **53**, 250 (2002)
33. K. Gesheva, A. Szekeres, T. Ivanova, Sol. Energy Mater. Sol. Cells **76**, 563 (2003)
34. P.M. Martin, Handbook of Deposition Technologies for Films and Coatings: Science, Applications and Technology (William Andrew, 2009)
35. K. Hinokuma, A. Kishimoto, T. Kudo, J. Electrochem. Soc. **141**, 876 (1994)
36. A. Guerfi, L.H. Dao, J. Electrochem. Soc. **136**, 2435 (1989)
37. M. Tubbs, Phys. Status Solidi A **21**, 253 (1974)
38. D. Pathak, R. Bedi, A. Kaushal, D. Kaur, Int. J. Mod. Phys. B **24**, 5379 (2010)
39. M.S. Burdis, J.R. Siddle, Thin Solid Films **237**, 320 (1994)
40. M.J. Davis, G. Benito, D.W. Sheel, M.E. Pemble, Chem. Vap. Deposition **10**, 29 (2004)
41. S. Ashraf, C.S. Blackman, G. Hyett, I.P. Parkin, J. Mater. Chem. **16**, 3575 (2006)
42. R.M. Guerrero, J.V. Garcia, V. Santes, E. Gomez, J. Alloys Compd. **434**, 701 (2007)

43. K. Khojier, H. Savaloni, S. Zolghadr, Appl. Surf. Sci. **320**, 315 (2014)
44. B.D. Cullity, Elements of X-ray Diffraction (Addison-Wesley Publishing, 1956)
45. J.M. Pachlhofer, C. Jachs, R. Franz, E. Franzke, H. Köstenbauer, J. Winkler, C. Mitterer, Vacuum **131**, 246 (2016)
46. S. Keshri, A. Kumar, D. Kabiraj, J. Nano- Electron. Phys. **3**, 260 (2011)
47. Y. Hiruta, M. Kitao, S. Yamada, Jpn. J. Appl. Phys. **23**, 1624 (1984)
48. R.J. Colton, A.M. Guzman, J.W. Rabalais, Acc. Chem. Res. **11**, 170 (1978)

Cite this article as: Danial Ahmad, M. Amer Khan, Arslan Mahmood, Amjad Sohail, S.S. Ali Gillani, Structural and optical properties of molybdenum oxide thin films prepared by the dip coating technique, Eur. Phys. J. Appl. Phys. **93**, 30301 (2021)